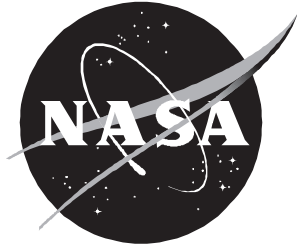NASA/TP-2000-210281

Materials for Low-Energy Neutron Radiation Shielding

Robert C. Singleterry, Jr., and Sheila A. Thibeault
Langley Research Center, Hampton, Virginia

June 2000

The NASA STI Program Office . . . in Profile

Since its founding, NASA has been dedicated to the advancement of aeronautics and space science. The NASA Scientific and Technical Information (STI) Program Office plays a key part in helping NASA maintain this important role.

The NASA STI Program Office is operated by Langley Research Center, the lead center for NASA's scientific and technical information. The NASA STI Program Office provides access to the NASA STI Database, the largest collection of aeronautical and space science STI in the world. The Program Office is also NASA's institutional mechanism for disseminating the results of its research and development activities. These results are published by NASA in the NASA STI Report Series, which includes the following report types:
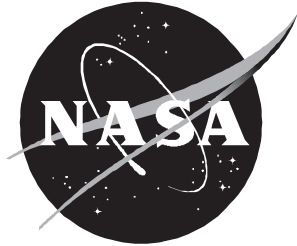
- TECHNICAL PUBLICATION. Reports of completed research or a major significant phase of research that present the results of NASA programs and include extensive data or theoretical analysis. Includes compilations of significant scientific and technical data and information deemed to be of continuing reference value. NASA counterpart of peer-reviewed formal professional papers, but having less stringent limitations on manuscript length and extent of graphic presentations.

- TECHNICAL MEMORANDUM. Scientific and technical findings that are preliminary or of specialized interest, e.g., quick release reports, working papers, and bibliographies that contain minimal annotation. Does not contain extensive analysis.

- CONTRACTOR REPORT. Scientific and technical findings by NASA-sponsored contractors and grantees.

- CONFERENCE PUBLICATION. Collected papers from scientific and technical conferences, symposia, seminars, or other meetings sponsored or co-sponsored by NASA.

- SPECIAL PUBLICATION. Scientific, technical, or historical information from NASA programs, projects, and missions, often concerned with subjects having substantial public interest.

- TECHNICAL TRANSLATION. English-language translations of foreign scientific and technical material pertinent to NASA's mission.

Specialized services that complement the STI Program Office's diverse offerings include creating custom thesauri, building customized databases, organizing and publishing research results . . . even providing videos.

For more information about the NASA STI Program Office, see the following:

- Access the NASA STI Program Home Page at *http://www.sti.nasa.gov*

- Email your question via the Internet to help@sti.nasa.gov

- Fax your question to the NASA STI Help Desk at (301) 621-0134

- Telephone the NASA STI Help Desk at (301) 621-0390

- Write to:
  NASA STI Help Desk
  NASA Center for AeroSpace Information
  7121 Standard Drive
  Hanover, MD 21076-1320

NASA/TP-2000-210281

Materials for Low-Energy Neutron Radiation Shielding

Robert C. Singleterry, Jr., and Sheila A. Thibeault
Langley Research Center, Hampton, Virginia

June 2000

Abstract

Various candidate aircraft and spacecraft materials were analyzed and compared in a low-energy neutron environment using the Monte Carlo N-Particle (MCNP) transport code with an energy range up to 20 MeV. Some candidate materials have been tested in particle beams, and others seemed reasonable to analyze in this manner before deciding to test them. The two metal alloys analyzed are actual materials being designed into or used in aircraft and spacecraft today. This analysis shows that hydrogen-bearing materials have the best shielding characteristics over the metal alloys. It also shows that neutrons above 1 MeV are reflected out of the face of the slab better by larger quantities of carbon in the material. If a low-energy absorber is added to the material, fewer neutrons are transmitted through the material. Future analyses should focus on combinations of scatterers and absorbers to optimize these reaction channels and on the higher energy neutron component (above 50 MeV).

1. Introduction

Ionizing radiation is a concern to the occupants and equipment of aircraft and spacecraft. The interior environment is modified from the ambient by the structure of the craft and its contents, which include the flight crew and passengers, if applicable. Therefore, the skin material and structure of the craft is an important component for determining the occupant and equipment radiation exposure along with its primary structural role.

Neutrons are generated when high-energy particles interact with matter. Because radiation sources for aircraft include the particles generated in the atmosphere above the aircraft, more neutrons exist in this situation than in a spacecraft environment. This fact does not mean that neutrons in the spacecraft environment are not important, just that a different modeling approach is needed because all the neutrons are generated in the spacecraft skin. Therefore, the focus of this paper is toward the aircraft environment.

The ambient radiation fields at most altitudes in the atmosphere are fairly weak, but the cumulative effect over the number of flight hours is where the concern lies. Also, as the flight altitudes increase for subsonic aircraft (47 000 to 55 000 ft) and especially for supersonic aircraft (60 000 to 70 000 ft), the ambient radiation levels increase and the flight crew, passengers, and electronic equipment become more susceptible to solar particle events.

Flight crew members are currently limited to 1000 flight hours per year, but passengers have no limits. To put this in perspective, current regulations for radiation workers allow nonpregnant personnel to receive 5 rem on an annual basis and the general public is limited to 0.1 rem in all situations. Recommendations are being considered (refs. 1 and 2) to lower the limit to 2 rem for nonpregnant radiation workers. It must be noted, however, that U.S. flight crews are not currently considered radiation workers. Therefore, they have no direct radiation exposure limits or monitoring requirements, just a limit of 1000 flight hours per year.

The high altitude, supersonic aircraft environment is also similar to the radiation environment measured at the surface of Mars. The density altitude of these aircraft is 20 to 25 g/cm^2, and the density altitude for the Martian surface is 20 to 25 g/cm^2. The constituent difference in the two atmospheres (air for Earth and CO_2 for Mars) is of little relevance. Therefore, any information gathered about high-altitude aircraft materials is applicable to materials needed for the habitation of Mars.

A large portion of the high-altitude radiation environment consists of neutrons (ref. 3). These neutrons appear mainly in two energy regions: a lower energy region between 0.1 and 10 MeV and a higher energy region between 50 and 1000 MeV. The low-energy neutrons are from an evaporation process where a neutron is boiled off from the nucleus because it contains an excess of energy from its last interaction. The high-energy neutrons occur from high-energy collisions

(ten's of GeV/nucleon) where the result of the interaction is a spray of nuclear fragments and particles.

The neutron evaporation spectrum has the same characteristics as a fission spectrum minus the gamma rays. Therefore, a standard nuclear reactor engineering model with experimentally derived interaction probabilities can be used to computationally test various materials in a fission spectrum to determine their neutron radiation modification characteristics. These results can then be used initially to evaluate, for the lower energy neutrons, various material combinations which can be compared with experimental data when available.

2. Material Selection and Simulation

The Monte Carlo N-Particle (MCNP) (ref. 4) program is used to simulate the particle interactions based on a Monte Carlo solution technique to the Boltzmann transport equation. The geometric model is a finite, plane-parallel slab, 3 g/cm^2 thick at 300 K. The source is an isotropic planar source at the left face of the slab and is modeled as an unmoderated Cf^{252} neutron source. Nine sample materials, enumerated in table 1, are each modeled as a single homogeneous slab. These nine materials represent structure or shielding materials currently being tested or materials that might be useful for structure or shielding but have never been analyzed or tested. The MCNP ID column lists the cross section sets used, which are the latest evaluated nuclear data file B (revision) (ENDF/B) evaluations available. This analysis method allows a comparison of the different materials without actually trying to model a specific component for a specific task. Important reaction channels can be identified within a material and an optimal shield can be designed to either encourage or discourage a particular channel through material selection and placement.

The aluminum alloy (No. 2024) is a standard light alloy being used in various aircraft and spacecraft structures. The titanium alloy (Ti6Al4V) is being considered for future high-altitude aircraft. The rest of the materials are a polymer-based carbon-fiber-reinforced epoxy composite (AS4/3502 graphite/epoxy composite) and polyethylene materials with various additives. The boronated polyethylene is a standard neutron absorber used in the nuclear industry. The beryllium and lithium additives are being investigated for their scattering and absorption properties.

The polymer-based composite material is being investigated for various reasons. First, these composites can be used as structural materials like aluminum and titanium. Second, they are lighter and therefore require less fuel to get to high altitudes and orbit. Finally, the reaction channels for nuclear fragmentation for the lighter elements in the shield are less numerous than for the heavier metal alloy elements. Therefore, the lighter materials should not create as many new particle fragments.

3. Results and Discussion

MCNP tallies were created to obtain the energy spectra for entrance and exit surface fluxes, total reaction rate, and elastic scattering and total absorption reaction rates in the slab material. Also, energy-integrated values of these tallies were created. With this information, a description of the differences among materials and why these differences occur can be formulated.

The source distribution is a typical Cf^{252} spectrum inherent in MCNP and is shown in figure 1. This source peaks at an energy of 2.5 MeV with its maximum energy on the order of 25 MeV. The evaporation spectrum of neutrons at high altitudes mimics this spectrum. Therefore, this source distribution can be used to approximate the evaporation spectrum that the materials in table 1 would encounter at high altitudes.

The energy spectra for the transmitted flux values are shown in figures 2 and 3 and are normalized by the Cf^{252} source flux from figure 1. From these spectra, the hydrogen-containing materials are seen to transmit fewer neutrons with energies above 100 keV than aluminum and titanium alloys; however, they transmit many more neutrons below 100 keV than even the source does. Fortunately, the biological damage (energy available to transmit to tissues) associated with these lower energy neutrons is small in comparison with those neutrons with energies above 100 keV.

The hydrogen-bearing materials reflect more low-energy neutrons than the metal alloys as shown in figures 4 and 5. Because the hydrogen nucleus (a proton) is approximately the same mass as the neutron, it is the

best neutron-scattering medium available and is the driving reaction channel for neutron reflection. An increase in the number of particles reflected out of a shield means the fewer particles that are available to affect tissues and cause biological damage. However, reflected neutrons from a vehicle in a space environment now act as a neutron source for extravehicular activities. This fact must be considered when something like the Space Station is being constructed by humans outside the vehicle.

Of the polyethylene-based materials, the pure material has the lowest transmission flux above 100 keV but the highest flux below 100 keV in both figures 2 and 3. This could be because the other materials have neutron scattering and absorption materials incorporated into their matrices displacing the hydrogen. The investigation of the reaction channels will clarify whether absorption or scattering (leakage) are causing these differences.

From the energy-integrated flux values listed in table 2, it is apparent that the hydrogen-rich materials also transmit the fewest total number of neutrons through the shield even though this is not apparent from figures 2 and 3. Additives to the basic polyethylene base have some effect on the integral shielding properties. For example, if an efficient neutron absorber is added, like B^{10}, then the total number of transmitted neutrons is reduced by another 10 percent.

The reflected flux is a measure of the total scattering properties of the material. Again, the more light elements in the material, the larger the integrated reflected flux will be. It is worth noting that of the polyethylene-based materials, the B^{10} material produced the smallest integrated reflected flux, probably because the number of neutrons available for the scattering reaction channel is reduced because of the high absorption. The metal alloys produce the smallest integrated reflected flux with the composite material between the two groups. The metal alloys are large atoms and are inefficient scattering materials. The composite material contains more carbon than hydrogen. Carbon is a good scatterer but not as efficient as hydrogen.

The spectral information in figures 4 and 5 shows the expected results and an unexpected one. Again, the polyethylene-based materials scatter the most neutrons to lower energies and allow them to backscatter out of

the material at those energies. However, for neutrons above 1 MeV, the aluminum alloy backscatters more neutrons than every other material except the composite. The larger titanium atoms would be expected to backscatter more than aluminum or the composite at those energies. However, the neutron absorption of the titanium alloy is much larger above 1 MeV than that of the composite or aluminum (ref. 5).

Figures 6 and 7 show the expected results for the total scattering reaction rate energy spectrum. At energies above 1 MeV, the titanium alloy shows a peak above all other materials because of the relatively large density of the titanium alloy compared with the other materials. However, the scattering reaction rate for both metal alloys drops very steeply as the energy of the neutron decreases because of the size of these atoms and the inability of these atoms to reduce the energy of the neutron per interaction. For large atoms, the energy reduction per interaction is small; therefore, the metal alloys do not scatter neutrons to the lower energies.

The hydrogen-containing materials, however, spread the neutron population over all energies in the spectrum because of the large average energy loss per interaction. The additives introduced into the hydrogenous material (boron, beryllium, and lithium) ultimately reduce the number of neutrons at the lower energies because of the reduced density of hydrogen in the materials and the absorption properties of the additives. The material that spreads more neutrons over all energies is pure polyethylene. This material is also the one with the largest hydrogen density. The composite material has the lowest hydrogen density, and even though neutrons are spread over all energies, the number of neutrons at the lower energies is an order of magnitude lower than for polyethylene.

Figures 8 and 9 show the total absorption reaction rates for the entire slab, which is important because it can keep neutrons from penetrating the shield and contributing to the dose of the occupants. These figures show typical absorption reaction rates for these materials. The metal alloys show many more resonance peaks over the spectrum than the hydrogenous materials. Also, the metal alloys do not scatter as many neutrons to lower energies; therefore the reaction rates decrease at the lower energies. Of the hydrogen-bearing materials, the materials with boron-10 and lithium-6 absorb many more neutrons than any of the

others. Also, these two materials show low-energy absorption peaks rather than a steady rise just because the flux increases at these energies. Therefore, these materials are demonstrating true absorption, instead of a flux-related absorption.

The reaction rates for (n,2n) and (n,3n) were so small, that they have not been included in this assessment. These reaction channels become much more important when the energy of the neutron becomes much larger (greater than 50 MeV).

Based on the foregoing analysis, pure polyethylene has the largest flux below 100 keV because it is the largest scatterer and smallest absorber of all the materials considered. Therefore, pure polyethylene is not considered to be the best choice for a shielding material. Borated polyethylene appears preferable, but a combination of various materials might outperform it. Clearly, considerable work remains yet to be done.

An interesting point to note is that the broad absorption resonance from boron (fig. 8) starting at about 100 keV does not overlap a pronounced peak from lithium at 300 keV (fig. 9). Also, the composite material is the best reflector of higher energy neutrons. These three materials could be combined together in a shield design to produce a better shield than any of them alone. Of course, the high-energy (greater than 50 MeV) response of this new shield would have to be analyzed to make sure these material additives do not increase the dose from their respective components.

4. Concluding Remarks

The hydrogen-bearing materials reduce the number of higher energy neutrons in the 500 keV to 20 MeV energy range that penetrate the shield materials considered. In fact, the more hydrogen, the better the overall shielding characteristics. These results also show that if neutron absorbers are added to the hydrogen-bearing material, then fewer neutrons penetrate the shield. If a polymeric composite material is added, then a better higher energy reflecting characteristic could be achieved. These results need to be extended and refined to design a shield material that can optimally shield for low-energy neutrons. This new shield then needs to be analyzed for the high-energy neutron component (greater than 50 MeV).

5. References

1. Anon.: *Limitation of Exposure to Ionizing Radiation*. NCRP Rep. No. 116, National Council on Radiation Protection and Measurements.

2. Anon.: *1990 Recommendations of the International Commission on Radiological Protection*. ICRP Publ. 60, Pergamon Press, 1991.

3. Wilson, John W.; Townsend, Lawrence W.; Schimmerling, Walter; Khandelwal, Govind S.; Khan, Ferdous; Nealy, John E.; Cucinotta, Francis A.; and Norbury, John W.: *Transport Methods and Interactions for Space Radiations*. NASA RP-1257, 1991.

4. Briesmeister, Judith F., ed.: MCNP—A General Monte Carlo N-Particle Transport Code, Version 4B, LA-12625-M, Version 4B, Los Alamos National Lab., 1997.

5. Singleterry, Robert C., Jr.; Shinn, Judy L.; Wilson, John W.; Maiden, Donald L.; Thibeault, Sheila A.; Badavi, Francis F.; Conroy, Thomas; and Braby, Leslie: *Aircraft Radiation Shield Experiments—Preflight Laboratory Testing*. NASA/TM-1999-209131, 1999.

Table 1. Elemental Compositions of Materials Analyzed

Material	Density, g/cm^3	Thickness, cm at 3 g/cm^2	Constituents	MCNP ID	Atomic fraction
2024 Al alloy	2.7	1.321586	Al-27	13027.60c	0.944469
			Li-7	03007.60c	0.035748
			Cu-63	29063.60c	0.011679
			Cu-65	29065.60c	0.005206
			Li-6	03006.60c	0.002899
Ti6Al4V alloy	4.46	0.672646	Ti-nat	22000.60c	0.876018
			Al-27	13027.60c	0.069090
			V-nat	23000.60c	0.054891
AS4/3502 graphite/epoxy composite	1.578	1.901141	C-nat	06000.60c	0.737823
			H-1	01001.60c	0.214368
			O-16	08016.60c	0.022268
			N-14	07014.60c	0.020364
			S-nat	16000.60c	0.005102
			N-15	07015.60c	0.000076
Polyethylene	0.91	3.296703	H-1	01001.60c	0.667954
			C-nat	06000.60c	0.332046
B^{10}-loaded polyethylene	0.92	3.26087	H-1	01001.60c	0.624741
			C-nat	06000.60c	0.310296
			B-10	05010.60c	0.064963
Be^9-loaded polyethylene	0.92	3.26087	H-1	01001.60c	0.624741
			C-nat	06000.60c	0.310296
			Be-9	04009.50c	0.064963
LiF-loaded polyethylene	1.13	2.654867	H-1	01001.60c	0.586502
			C-nat	06000.60c	0.290897
			F-19	09019.60c	0.061286
			Li-7	03007.60c	0.056203
			Li-6	03006.60c	0.005112
Li$_2$CO$_3$-loaded polyethylene	1.06	2.830189	H-1	01001.60c	0.533709
			C-nat	06000.60c	0.298219
			O-16	08016.60c	0.101086
			Li-7	03007.60c	0.061392
			Li-6	03006.60c	0.005584
Li$_2^6$CO$_3$-loaded polyethylene	1.08	2.777778	H-1	01001.60c	0.527656
			C-nat	06000.60c	0.295406
			O-16	08016.60c	0.100132
			Li-6	03006.60c	0.076806

Table 2. Energy Integrated Transmitted and Reflected Neutron Flux From Each Material per Source Neutron

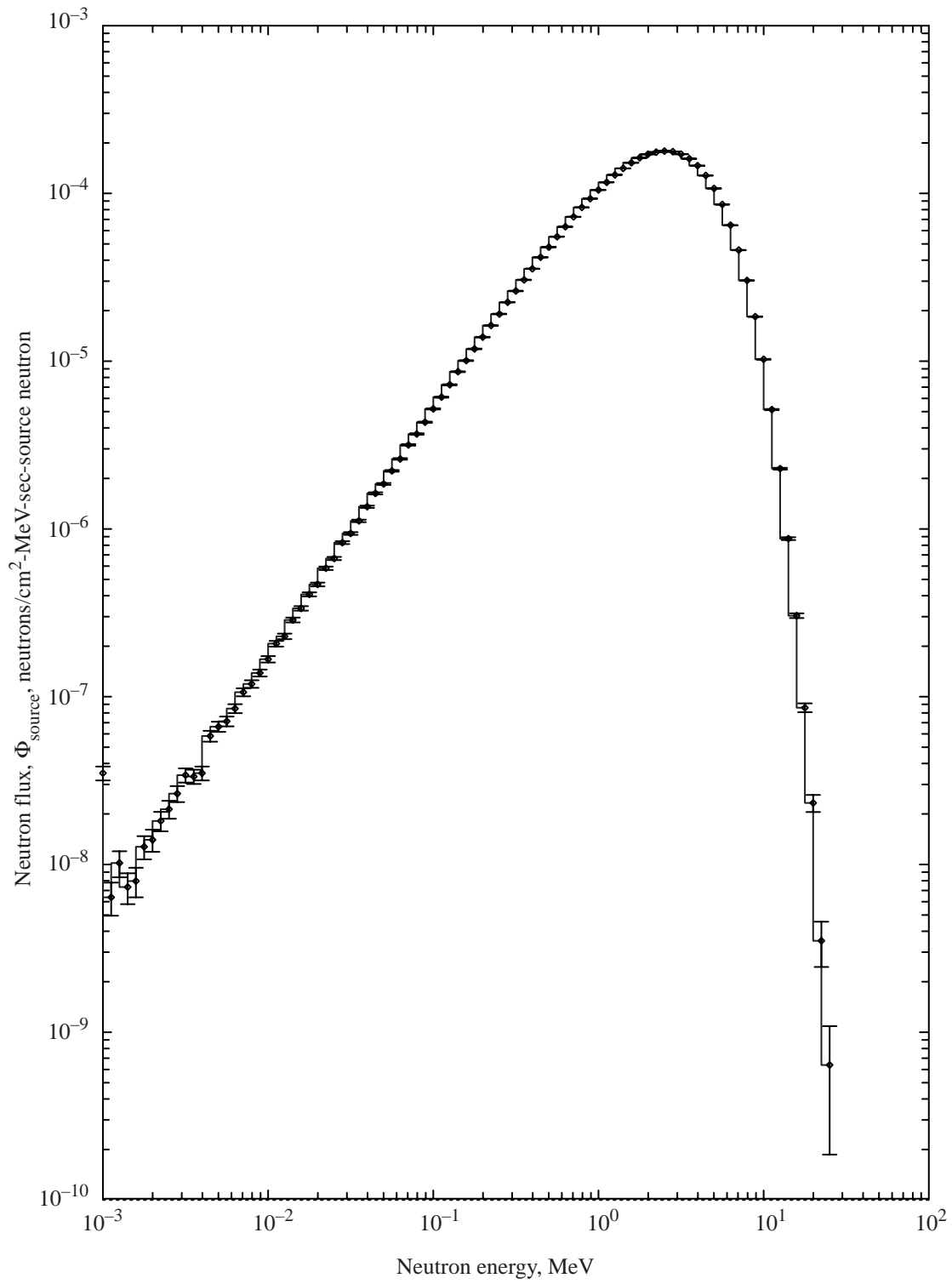| Material ID	Transmitted flux neutrons/cm^2-sec-source	Reflected flux neutrons/cm^2-sec-source
Source	4.302×10^{-2}	
2024 Al alloy	1.904×10^{-2}	4.946×10^{-2}
Ti6Al4V alloy	2.249×10^{-2}	4.848×10^{-2}
AS4/3502 composite	1.381×10^{-2}	5.182×10^{-2}
Polyethylene	0.962×10^{-2}	5.361×10^{-2}
B^{10} PE	0.850×10^{-2}	5.187×10^{-2}
Be^9 PE	0.994×10^{-2}	5.357×10^{-2}
LiF PE	1.022×10^{-2}	5.285×10^{-2}
Li$_2$CO$_3$ PE	1.088×10^{-2}	5.270×10^{-2}
Li$_2^6$CO$_3$ PE	1.041×10^{-2}	5.221×10^{-2}

Figure 1. Cf^{252} source neutron energy spectrum.
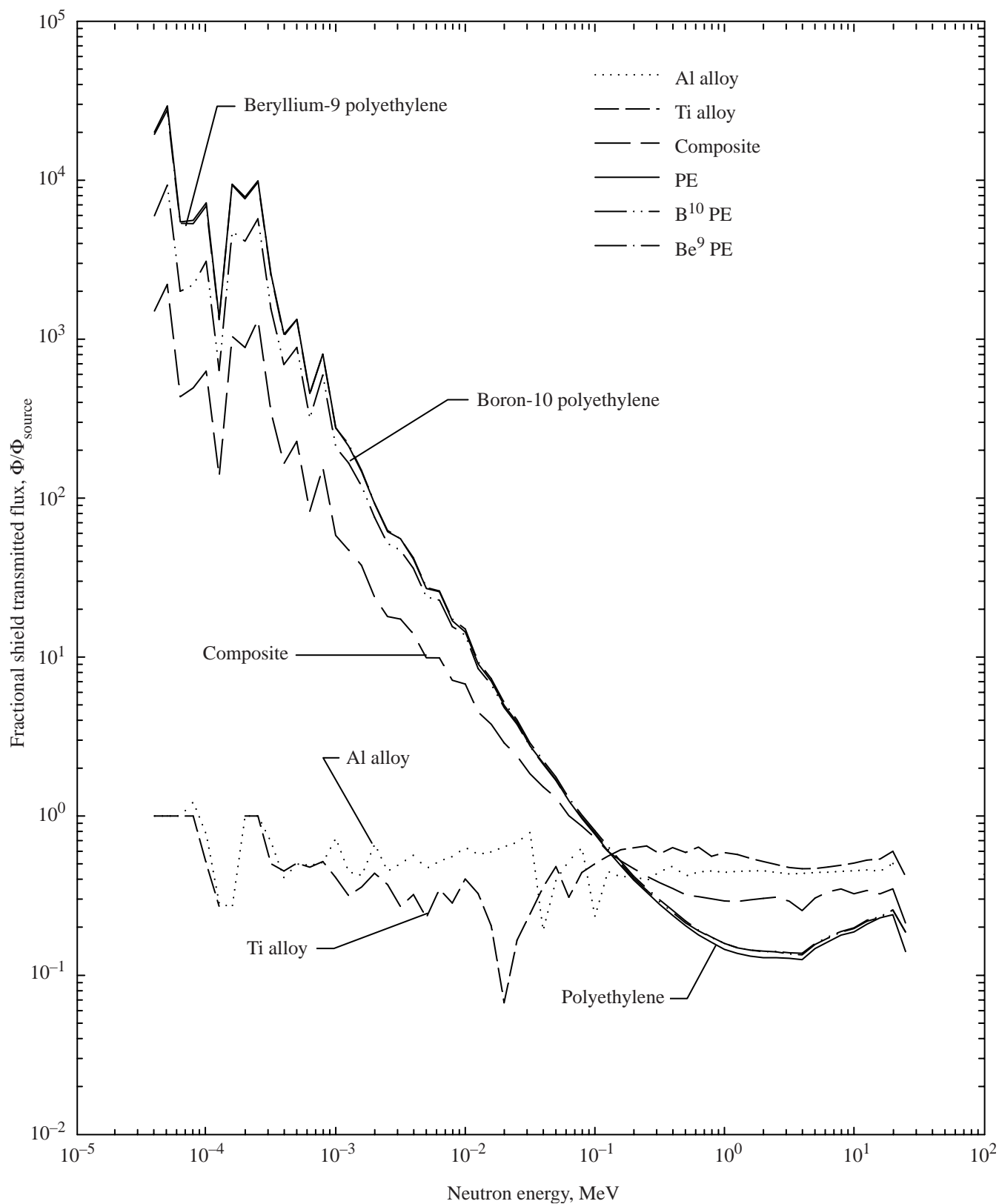
Figure 2. Normalized neutron energy spectrum for transmission flux for four reference materials and for boron- and beryllium-containing materials.
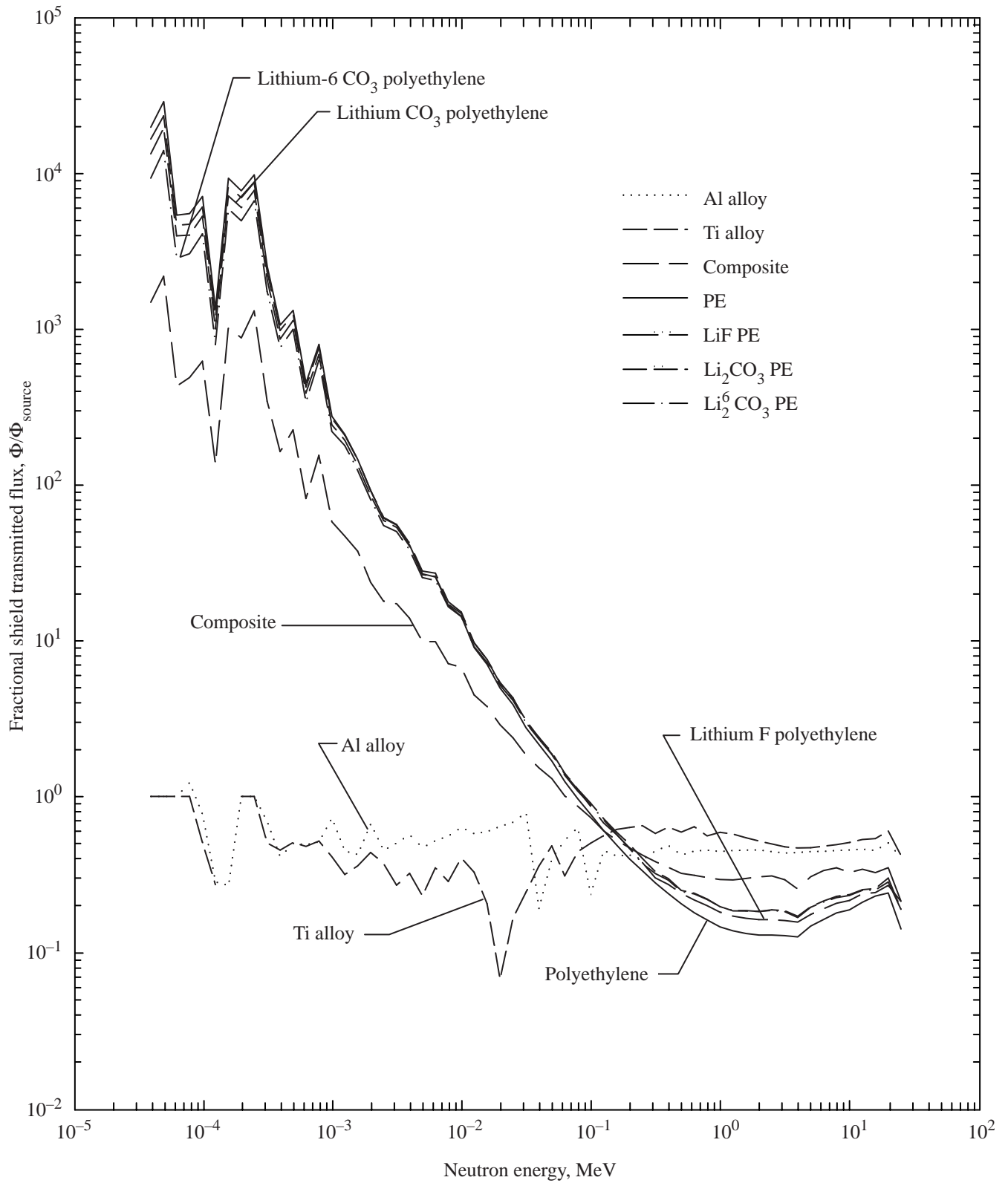
Figure 3. Normalized neutron energy spectrum for transmission flux for four reference materials and for various lithium-containing materials.
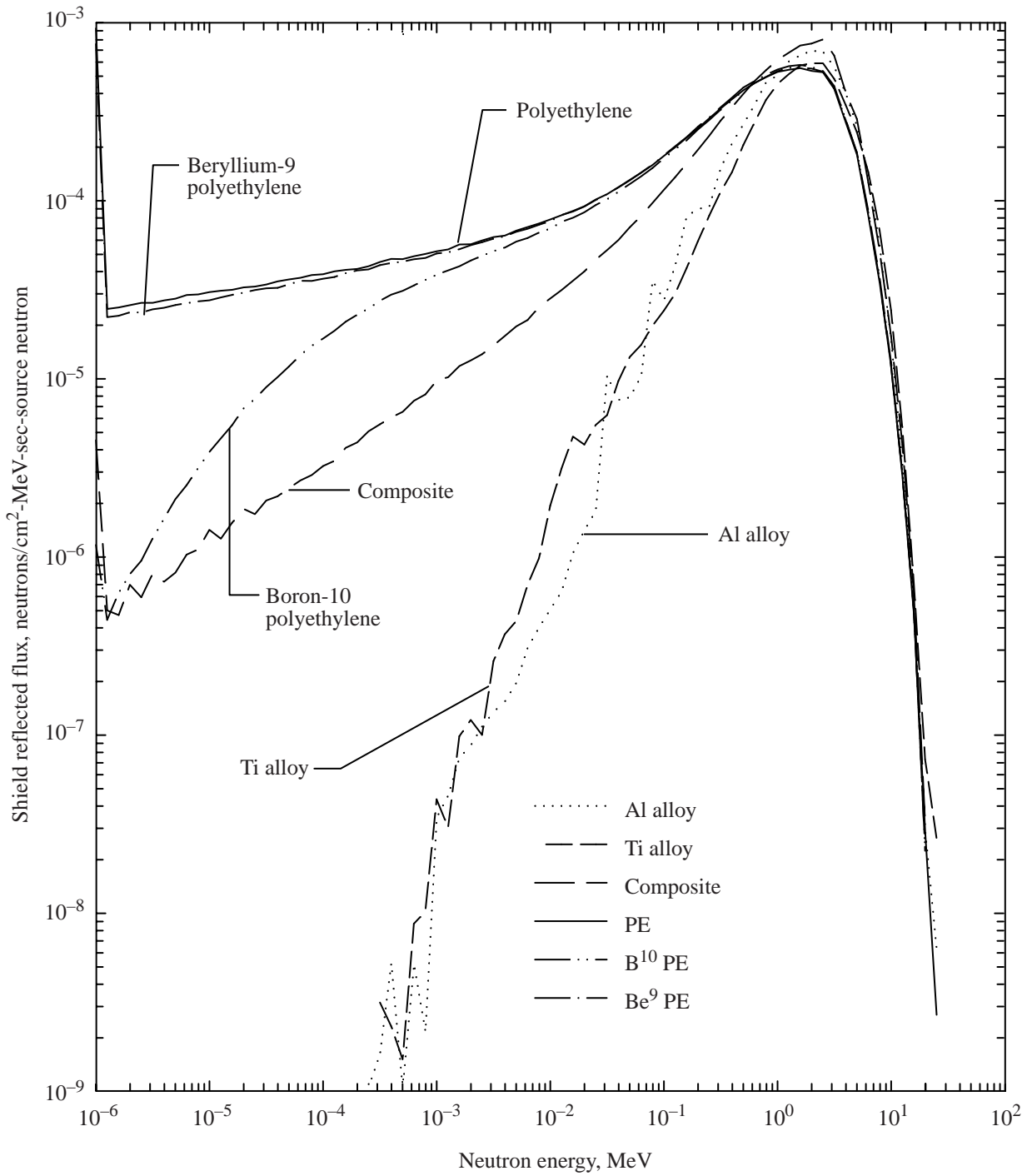
Figure 4. Neutron energy spectrum for reflected flux for four reference materials and for boron- and beryllium-containing materials.
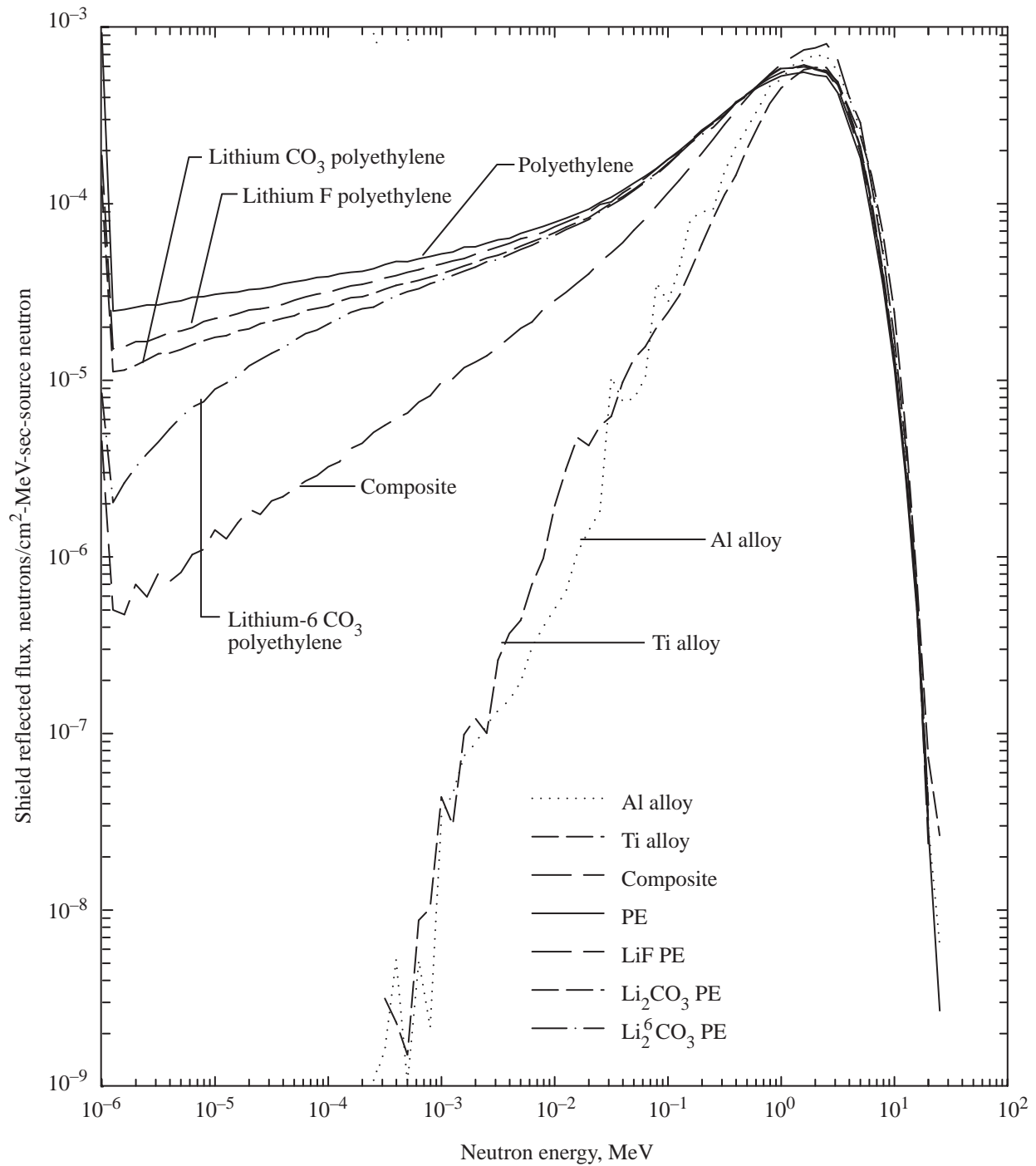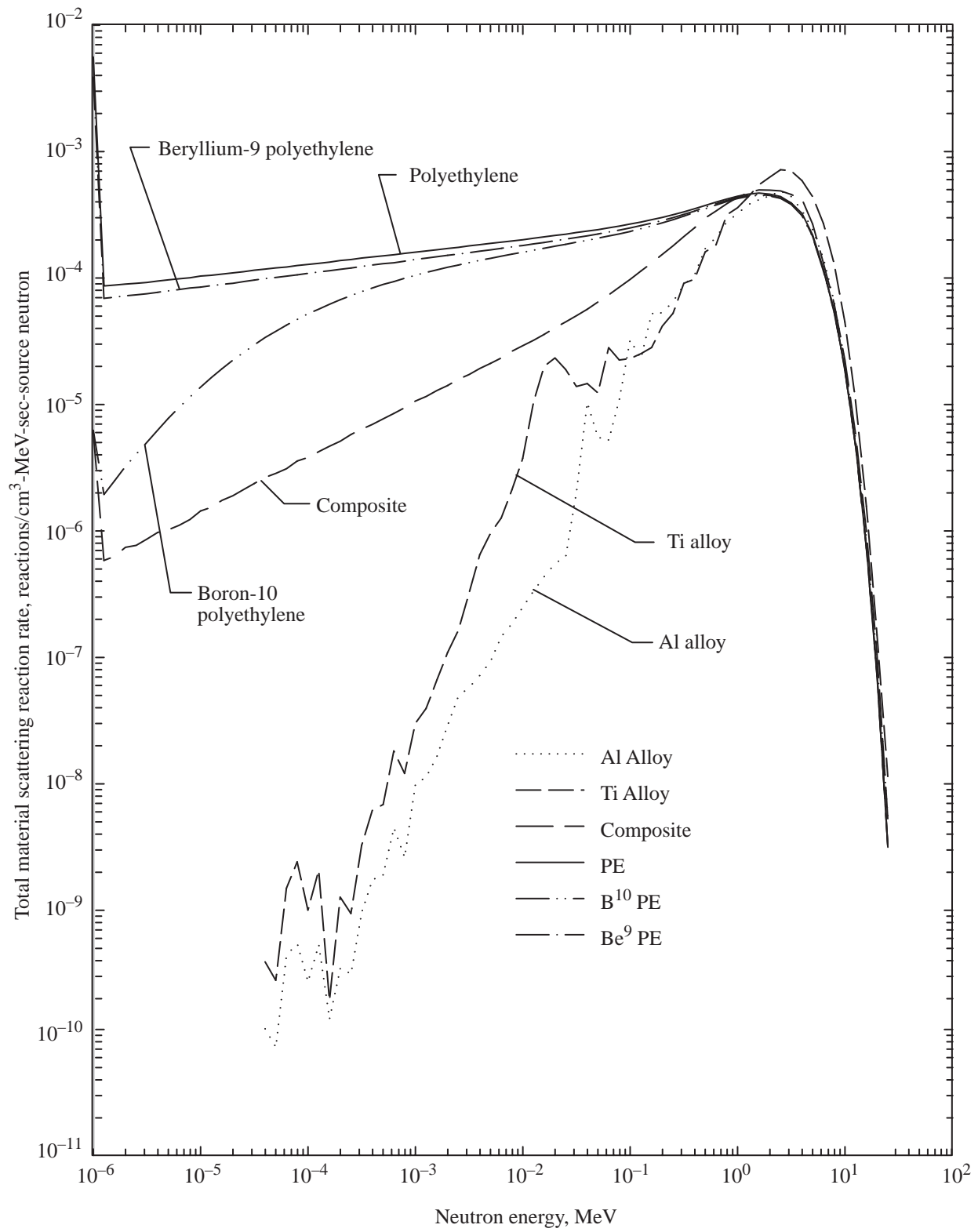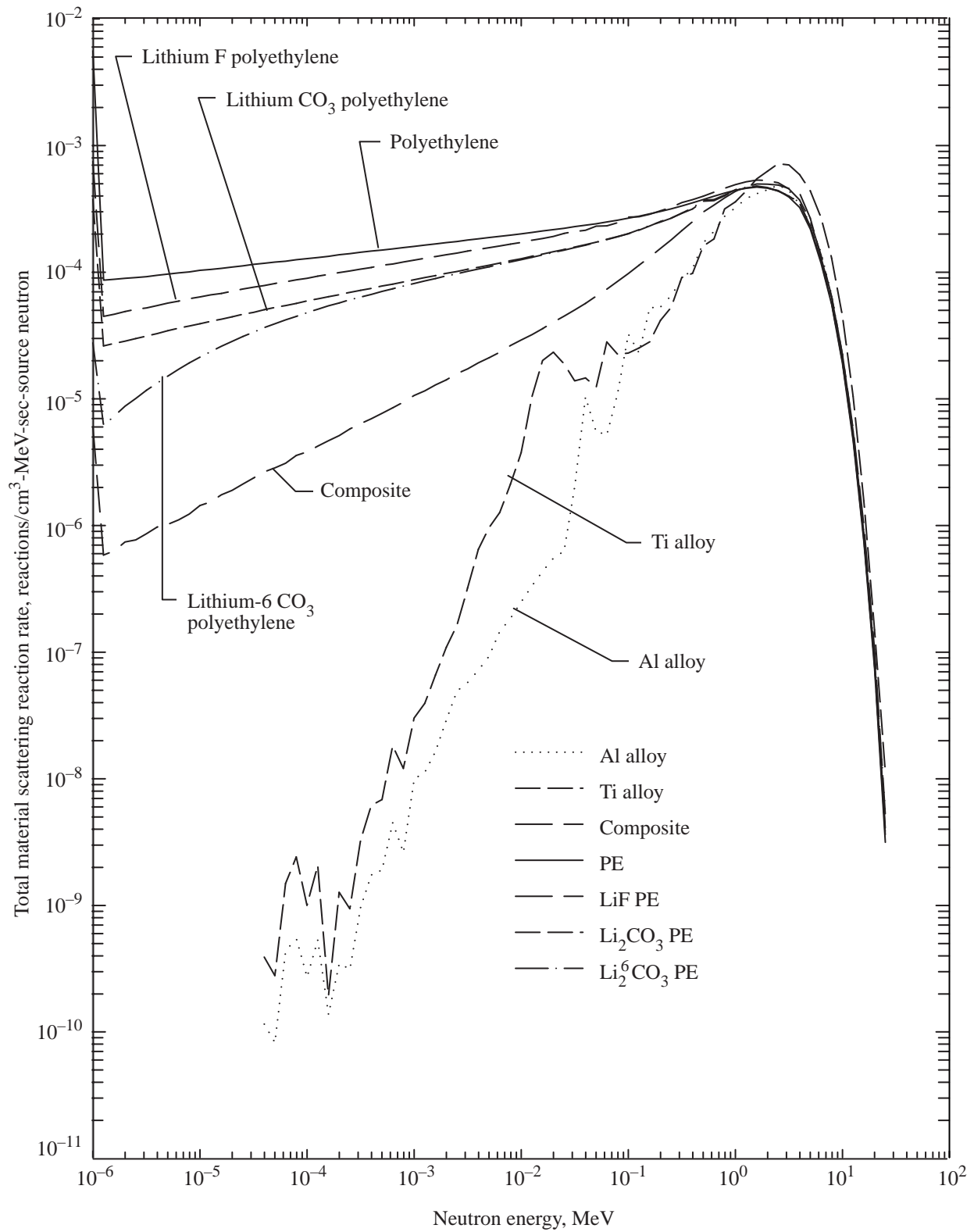
Figure 5. Neutron energy spectrum for reflected flux for four reference materials and for various lithium-containing materials.
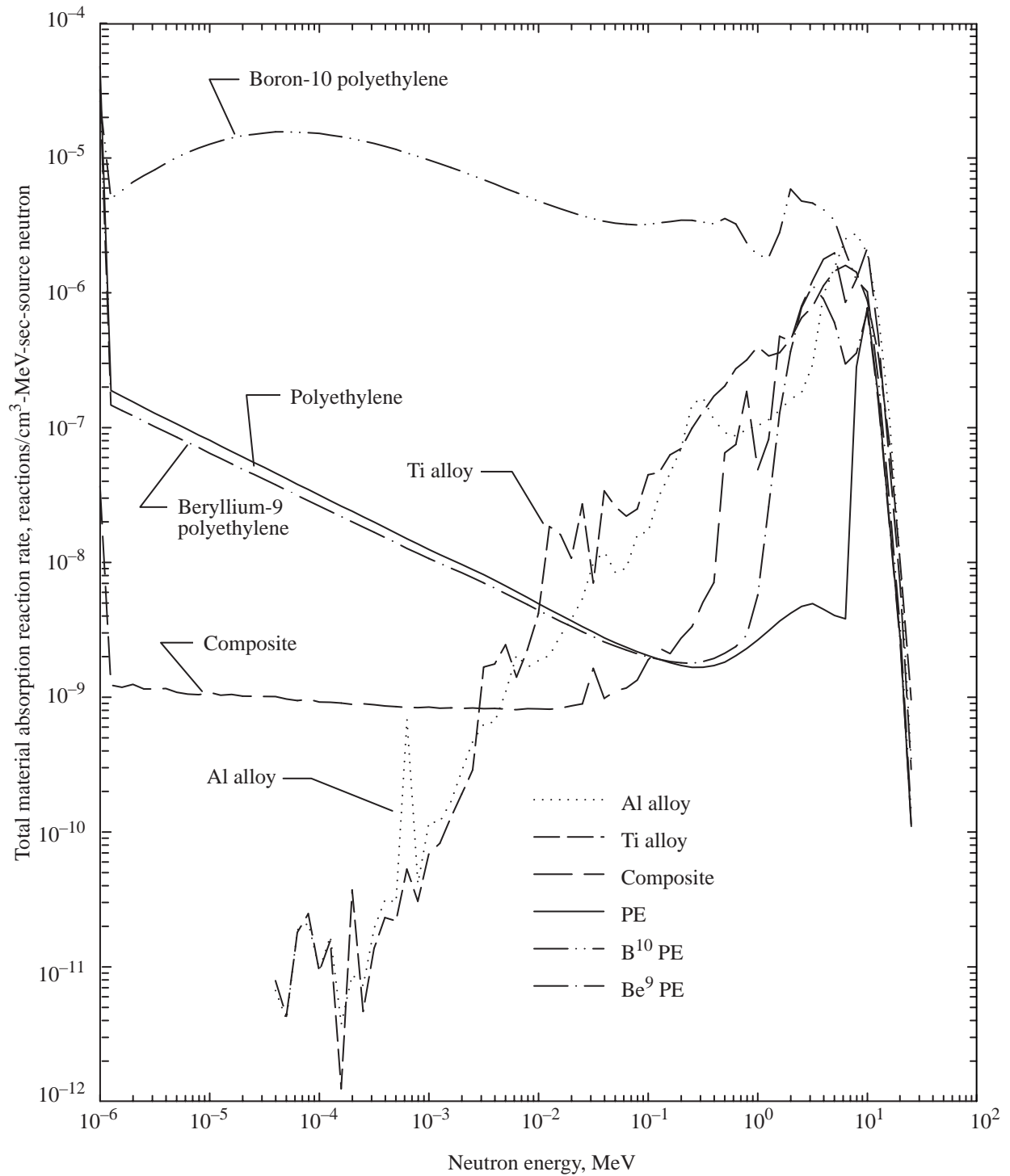
Figure 6. Neutron energy spectrum for total scattering reaction rate for four reference materials and for boron- and beryllium-containing materials.
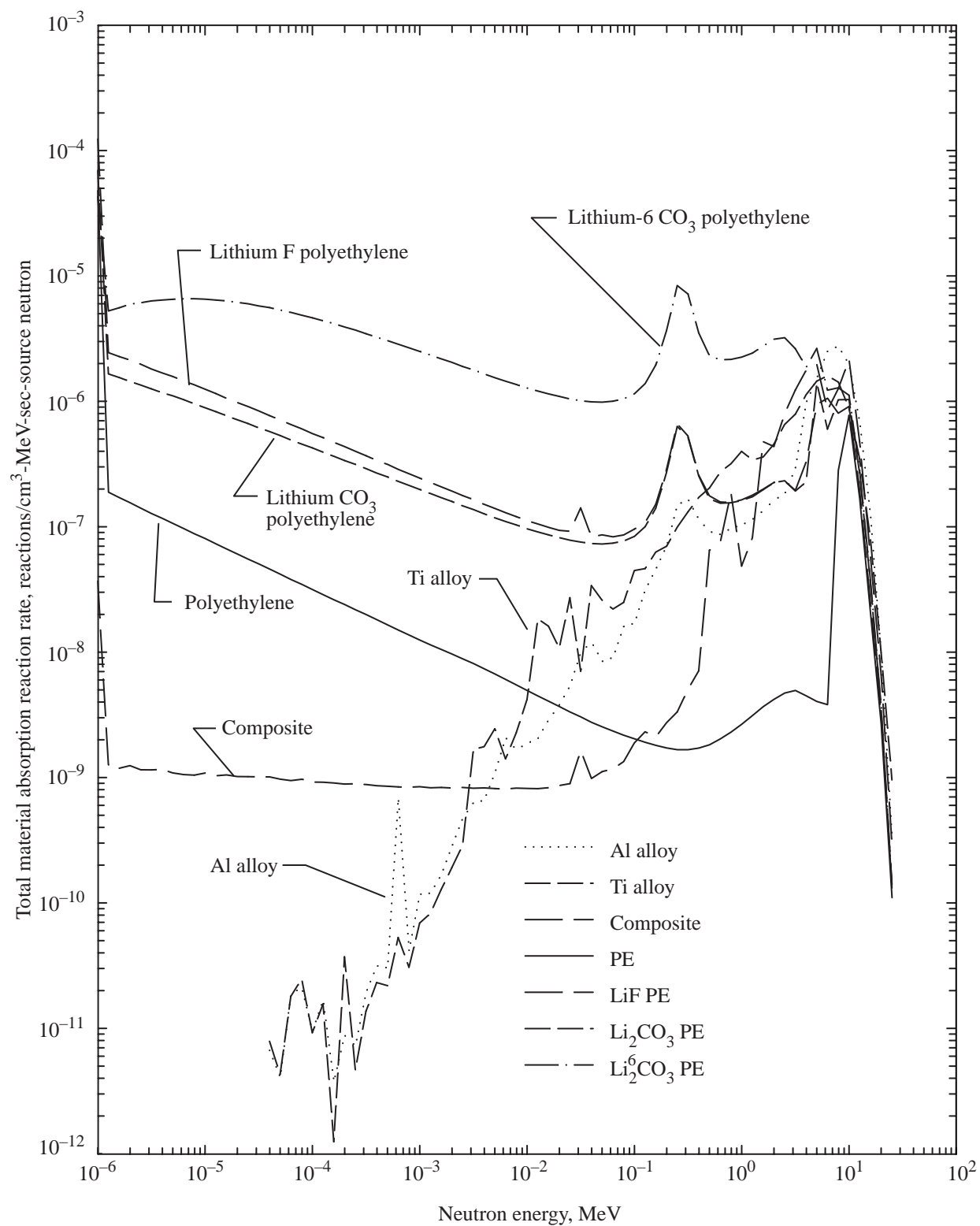
Figure 7. Neutron energy spectrum for total scattering reaction rate for four reference materials and for various lithium-containing materials.

Figure 8. Neutron energy spectrum for total absorption reaction rate for four reference materials and for boron- and beryllium-containing materials.

Figure 9. Neutron energy spectrum for total absorption reaction rate for four reference materials and for various lithium-containing materials.

1. AGENCY USE ONLY *(Leave blank)*	2. REPORT DATE June 2000	3. REPORT TYPE AND DATES COVERED Technical Publication	
4. TITLE AND SUBTITLE Materials for Low-Energy Neutron Radiation Shielding		**5. FUNDING NUMBERS** WU 101-15-01-51	
6. AUTHOR(S) Robert C. Singleterry, Jr., and Sheila A. Thibeault			
7. PERFORMING ORGANIZATION NAME(S) AND ADDRESS(ES) NASA Langley Research Center Hampton, VA 23681-2199		**8. PERFORMING ORGANIZATION REPORT NUMBER** L-17773	
9. SPONSORING/MONITORING AGENCY NAME(S) AND ADDRESS(ES) National Aeronautics and Space Administration Washington, DC 20546-0001		**10. SPONSORING/MONITORING AGENCY REPORT NUMBER** NASA/TP-2000-210281	
11. SUPPLEMENTARY NOTES			
12a. DISTRIBUTION/AVAILABILITY STATEMENT Unclassified–Unlimited Subject Category 93 Distribution: Standard Availability: NASA CASI (301) 621-0390		**12b. DISTRIBUTION CODE**	

13. ABSTRACT *(Maximum 200 words)*

Various candidate aircraft and spacecraft materials were analyzed and compared in a low-energy neutron environment using the Monte Carlo N-Particle (MCNP) transport code with an energy range up to 20 MeV. Some candidate materials have been tested in particle beams, and others seemed reasonable to analyze in this manner before deciding to test them. The two metal alloys analyzed are actual materials being designed into or used in aircraft and spacecraft today. This analysis shows that hydrogen-bearing materials have the best shielding characteristics over the metal alloys. It also shows that neutrons above 1 MeV are reflected out of the face of the slab better by larger quantities of carbon in the material. If a low-energy absorber is added to the material, fewer neutrons are transmitted through the material. Future analyses should focus on combinations of scatterers and absorbers to optimize these reaction channels and on the higher energy neutron component (above 50 MeV).

14. SUBJECT TERMS Neutron shielding; Radiation; Materials comparison; High altitude			**15. NUMBER OF PAGES** 19
			16. PRICE CODE A03
17. SECURITY CLASSIFICATION OF REPORT Unclassified	**18. SECURITY CLASSIFICATION OF THIS PAGE** Unclassified	**19. SECURITY CLASSIFICATION OF ABSTRACT** Unclassified	**20. LIMITATION OF ABSTRACT** UL